A Model for the Evolution of Biological Specificity: a Cross-Reacting DNA-Binding Protein Causes Plasmid Incompatibility

JB
Journals.ASM.org

A Model for the Evolution of Biological Specificity: a Cross-Reacting DNA-Binding Protein Causes Plasmid Incompatibility

Edel M. Hyland,[a]* Edward W. J. Wallace,[b] Andrew W. Murray[a]

FAS Center for Systems Biology, Harvard University, Cambridge, Massachusetts, USA[a]; Department of Biochemistry and Molecular Biology, University of Chicago, Chicago, Illinois, USA[b]

Few biological systems permit rigorous testing of how changes in DNA sequence give rise to adaptive phenotypes. In this study, we sought a simplified experimental system with a detailed understanding of the genotype-to-phenotype relationship that could be altered by environmental perturbations. We focused on plasmid fitness, i.e., the ability of plasmids to be stably maintained in a bacterial population, which is dictated by the plasmid's replication and segregation machinery. Although plasmid replication depends on host proteins, the type II plasmid partitioning (Par) machinery is entirely plasmid encoded and relies solely on three components: *parC*, a centromere-like DNA sequence, ParR, a DNA-binding protein that interacts with *parC*, and ParM, which forms actin-like filaments that push two plasmids away from each other at cell division. Interactions between the Par operons of two related plasmids can cause incompatibility and the reduced transmission of one or both plasmids. We have identified segregation-dependent plasmid incompatibility between the highly divergent Par operons of plasmids pB171 and pCP301. Genetic and biochemical studies revealed that the incompatibility is due to the functional promiscuity of the DNA-binding protein $ParR_{pB171}$, which interacts with both *parC* DNA sequences to direct plasmid segregation, indicating that the lack of DNA binding specificity is detrimental to plasmid fitness in this environment. This study therefore successfully utilized plasmid segregation to dissect the molecular interactions between genotype, phenotype, and fitness.

In recent years, there has been appreciable progress in linking adaptive phenotypes to specific genetic alterations (reviewed in reference 1), thus shedding light on the molecular details of evolution. Two challenges, however, make it difficult to rigorously link mutations, through changes in biochemistry and cell biology, to gains in fitness: the complexity of living systems makes it difficult to define all the phenotypic outcomes of a given mutation, and accurate measurement of fitness in environments in which organisms have evolved is not always achievable. We therefore sought a simplified experimental system with a detailed understanding of the genotype-to-phenotype relationship that could be altered by environmental perturbations.

We focused specifically on the interactions between two proteins and one protein-binding DNA sequence that direct the segregation of a class of bacterial plasmids. Most plasmids are maintained at low copy numbers, and their successful transmission depends on regulated DNA replication and segregation mechanisms that ensure that each daughter cell receives at least one copy of the plasmid. Filament-driven plasmid segregation ensures accurate plasmid transmission at cell division, and unlike plasmid replication systems, this stabilization mechanism is completely plasmid encoded and, as far as we know, does not rely on host proteins. We utilized the type II partitioning (Par) system, first described for the R1 plasmid from *Salmonella enterica* (2), which relies on three components, all carried or encoded on a single operon (3): a centromere-like DNA sequence, *parC*, and two proteins, ParR (NP_957569.1), a DNA-binding protein that interacts with *parC*, and ParM (NP_957570.1), an ATPase that forms an actin-like filament (4–7). The binding of ParR to *parC* creates a complex that protects ParM filaments from depolymerization, and the growth of a filament between two plasmids can segregate them to either end of a rod-shaped cell, thus ensuring that each daughter receives at least one plasmid copy (8–10). The detailed analysis of the R1 Par operon is a framework to interpret the partitioning systems of other Par operons (11).

Interactions between genes and environments control the fitness of genotypes. We used incompatibility to manipulate the environment in which Par operons functioned. Two plasmids are compatible if the presence of one has no effect on the inheritance of the other and are incompatible if each interferes with the replication or segregation of the other. In our experimental system, we used compatible replication origins to focus attention on the role of the Par operon in incompatibility. The mixed-filament model for partitioning incompatibility hypothesizes that the elongation of one ParM filament with two different plasmids at each of its ends impairs the inheritance of both plasmids, eventually generating subpopulations of bacterial cells that contain only one of the two plasmids (reviewed in reference 12).

To study the evolution of biological specificity, we investigated the mechanism of segregation-dependent plasmid incompatibility. It has previously been shown that such incompatibility between the elements of a type 1 ParA/ParB segregation system is dictated by "discriminator contacts" between the centromere-like *parS* DNA sequence and the DNA-binding protein ParB (13, 14). In this study, we tested the compatibility of seven type II Par oper-

Received 23 May 2014 Accepted 5 June 2014
Published ahead of print 9 June 2014
Address correspondence to Edel M. Hyland, ehyland1@gmail.com.
* Present address: Edel M. Hyland, School of Biotechnology, Dublin City University, Dublin, Ireland.
Supplemental material for this article may be found at http://dx.doi.org/10.1128/JB.01811-14.

doi:10.1128/JB.01811-14

ons and detected strong incompatibility between two, namely, those from plasmids pB171 (NC_002142.1) (15) and pCP301 (NC_004851.1) (16), despite the substantial sequence divergence of their Par operons. Our experimental data have shown that ParR from pB171 ($ParR_{pB171}$) binds to the *parC* sequence from both plasmids and that both interactions can direct plasmid segregation. Furthermore, our mathematical model supports the hypothesis that this molecular cross-reaction is the underlying mechanism that leads to plasmid incompatibility, consistent with the results found for the type I segregation system. This report therefore illuminates how genotype, phenotype, and environment interact to contribute to the success of a simple genetic element.

MATERIALS AND METHODS

Bacterial strains and plasmid construction. *Escherichia coli* strain DH5α [*fhuA2 lac*(*del*)*U169 phoA glnV44* Φ80′ *lacZ*(*del*)*M15 gyrA96 recA1 relA1 endA1 thi-1 hsdR17*] was utilized in all experiments and manipulated using standard microbiology techniques. Plasmid construction details are in the supplemental material. Table S2 in the supplemental material summarizes the names and important features of all plasmids used in this study.

Plasmid stability and incompatibility assays. DH5α cells were transformed with the pEMH606-derived resident plasmid and selected on chloramphenicol (Cm) plates. For qualitative plasmid stability assays, single transformants were grown to saturation in selective media, and 10^9 cells were plated directly onto LB plates containing 20 μg/ml X-Gal (5-bromo-4-chloro-3-indoyl-β-D-galactopyranoside) and incubated at 30°C for 3 to 4 days. Colonies were photographed without magnification. For quantitative plasmid stability assays, transformants were grown under selective conditions (LB plus Cm) to saturation and rediluted 10,000-fold into fresh media every 24 h, for 5 days, producing approximately 70 generations. Typically, on days 3, 4, and 5, cultures were sampled and plated onto (i) LB plates (nonselective) and (ii) LB-plus-Cm plates (selecting for plasmid). The counts on both plates were modeled as Poisson random variables with means as follows:

$$E(y_{cgi}) = V_{cgi}\,\sigma_{cg}$$

$$E(x_{cgi}) = V_{cgi}\,\sigma_{cg}\,(1 - l)^g$$

where y_{cgi} represents the observed cell count on nonselective plate *i* from culture *c* at generation *g*, x_{cgi} represents the observed cell count on selective plate *i* from culture *c* at generation *g*, V_{cgi} represents the volume of the plated sample on plate *i* from culture *c* at generation *g*, ρ_{cg} represents the cell density in culture *c* at generation *g*, and *l* represents the plasmid loss rate per generation.

Loss rate l was the parameter of interest; the generalized linear model framework, also known as a Poisson regression, gives joint maximum-likelihood estimates of *l* and ρ_{cg}, pooling information from samples taken across multiple time points (generations). As a nuisance parameter, ρ_{cg} was not reported. Estimates were made with the *glm* function in R (17).

For incompatibility tests, cells were initially transformed with the pEMH606-derived, low-copy-number "resident plasmid." These cells were transformed using the high-copy-number (*ori*MB1) "challenge plasmid" carrying the kanamycin (Kan) resistance gene and were selected on LB-plus-Cm-plus-Kan plates. Individual transformants were grown for 90 min in doubly selective media (LB plus Cm plus Kan) and then transferred to LB plus Kan, which selects only for the challenge plasmid. Cultures were propagated and sampled for 70 generations, as described above. The loss rate of the resident plasmid was estimated by the maximum-likelihood method as detailed above using colony counts from LB-plus-Kan and LB-plus-Cm-plus-Kan plates.

For the half-sectored plasmid stability assay, cells were grown to saturation under selective conditions. Cultures were diluted and plated for single colonies on media containing X-Gal under nonselective conditions. Plates were incubated at 30°C for 2 days, and the half-sectored phenotype was scored for at least 500 colonies per plasmid tested.

Note on the plasmid incompatibility assay. Fluctuations in resident plasmid copy number influence the loss rates detected for incompatibility assays. During the course of this work, it was brought to our attention that plasmid copy numbers are influenced by the growth phase of a bacterial culture (18, 19) and, therefore, that the length of time each culture is maintained in saturation impacts incompatibility levels. The data presented in each individual figure in this article were collected on the same day; therefore, the loss rates of all samples represented within the same figure can be directly compared. However, because experiments were not controlled for the length of time cultures were maintained at saturation between dilutions, quantitative differences between figures in loss rates reported are less reliable.

Red fluorescent protein (RFP) reporter assays. DH5α cells were transformed with 2 independent clones of each plasmid containing the *parC* mKate fluorescence reporter construct. Three colonies were selected from each transformation plate and grown under selective conditions in the presence of ampicillin to the exponential phase. Fluorescence was monitored for each cell population using an LSRII flow cytometer (BD Biosciences) and mean fluorescence recorded.

Electrophoretic mobility shift assays. *parC* DNA sequences were amplified and purified on mini-spin columns (Qiagen, Limburg, Holland); $parC_{pCP301}$ was amplified from pEMH608 with oEMH414 and oEMH294, $parC_{pB171}$ was amplified from pEMH617 with oEMH314 and oEMH294, and $parC_{R1}$ was amplified from pEMH607 with oEMH548 plus oEMH294 and pUC18-derived DNA using primers oEMH549 and oEMH329. Purified ParR proteins were diluted in binding buffer ($ParR_{pB171}$ binding buffer, 10 mM Tris-Cl [pH 7.5], 50 mM NaCl, 50 mM KCl, 1 mM EDTA [pH 8.0], 1 mM dithiothreitol [DTT], 2 mM $MgCl_2$; $ParR_{pCP301}$ binding buffer, 10 mM Tris-Cl [pH 7.5], 50 mM KCl, 1 mM EDTA [pH 8.0], 1 mM DTT, 2 mM $MgCl_2$, 10% glycerol). *parC* DNA (2 nM) was incubated with increasing concentrations of ParR proteins in a final reaction volume of 15 μl, and binding was allowed to proceed for 30 min at room temperature. Gel loading buffer was added to each reaction, and the complete volume of each sample was loaded onto prerun 7.5% Tris-Cl gels (Bio-Rad). Gels were run at 80 V for 3 h at 4°C, and DNA was visualized by staining gels with SYBR green stain (Invitrogen) for 20 min and scanning stained gels on a Typhoon scanner (excitation wavelength of 488 nm and visualization parameters compatible with Alexa Fluor 488 dyes).

Simulating plasmid segregation. The detailed model for our simulations is described in the supplemental material. We used first-order chemical kinetics to model association and dissociation of *parC* and preformed ParR complexes, making the assumptions that ParR and *parC* binding was slow relative to the capture of these complexes by ParM filaments and elongation of ParM filaments and that each ParR complex that was bound to DNA associated only with its homologous ParM filaments. The simulation was performed using Gillespie's stochastic simulation algorithm and a stimulation period that was long enough to ensure that the last state of a dividing cell was sampled from the steady-state distribution of plasmids and filaments. When a cell divided, all the plasmids that were associated with one type of ParR were equally partitioned between the two daughter cells; if the number of plasmids was odd, the last plasmid was randomly assigned to one of the daughters. All the plasmids that had not associated with ParR were randomly assigned to daughter cells, mimicking binomial partition. All ParR and *parC* complexes were assumed to form at the same rate, and their dissociation rates were estimated from analyzing the ability of ParR to inhibit the expression of fluorescent proteins from *parC*.

His-tagged ParR protein purification. BL21(DE3) cells were transformed with C-terminally His-tagged $ParR_{pB171}$ (pEMH535) or $ParR_{pCP301}$(pEMH536) plasmids. A single transformant from each plate was grown to saturation in selective media and was used to inoculate 1.5 liters of fresh LB media. This culture was grown at 37°C to final optical

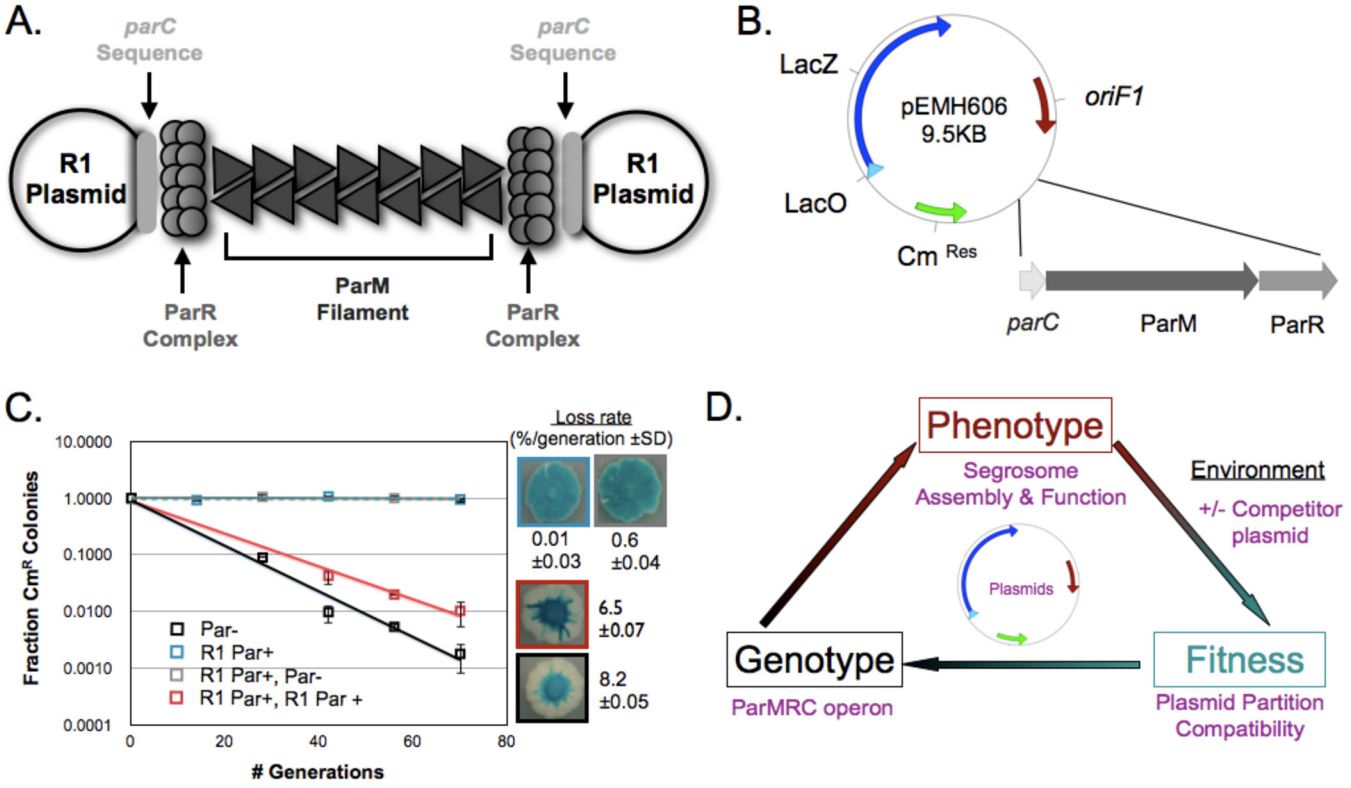

FIG 1 Establishing a plasmid system, based on plasmid partitioning, to study molecular adaptation. (A) Schematic of the structure of a functional example of R1 partition machinery: the molecular machine encoded by the Par operon that separates two R1 plasmids. (B) Map of the low-copy-number mini-F1 plasmid, pEMH606, which served as the backbone of the resident plasmids, showing the presence of chloramphenicol resistance (Cm^{Res}) and β-galactosidase (LacZ) genes, the origin of replication, *oriF1*, and the location where the type II partitioning operons were inserted. (C) Qualitative and quantitative plasmid stability and incompatibility assays to monitor (i) the ability of the R1 Par operon (blue) to stabilize pEMH606 (black) and (ii) the destabilization of a resident plasmid, made by cloning the R1 Par operon into pEMH606, by a high-copy-number challenge plasmid that also carries the R1 Par operon (red). Error bars represent the 95% confidence intervals derived from two biological replicates, assayed in triplicate, and loss rates are provided with standard deviations (SD). (D) The relationship between genotype, phenotype, and fitness of the plasmid segregation system.

densities at 600 nm (OD_{600}) of ~0.65 ($ParR_{pCP301}$) and ~0.4 ($ParR_{pB171}$) and then transferred to 18°C. After 15 min, protein expression was induced by the addition of 0.4 mM IPTG (isopropyl-β-D-thiogalactopyranoside) and the culture was incubated for a further 20 h. Cells were pelleted at 3,000 × *g* for 20 min and stored overnight at −80°C. Cells were thawed on ice and resuspended in 30 ml lysis buffer (50 mM Tris-Cl [pH 9.0], 400 mM KCl, 1 mM phenylmethylsulfonyl fluoride [PMSF], 0.05% β-mercaptoethanol; for $ParR_{pCP301}$, pH 9.0; for $ParR_{pB171}$, pH 8.0). Benzonase (Sigma, MO) was added to reach a final concentration of 100 U/ml, and a French press was used to lyse the cells. The lysate was collected by centrifugation at 30,000 × *g* for 1 h and was incubated with a 2-ml bed volume of nickel-nitrilotriacetic acid (Ni-NTA) resin (Qiagen, Limburg, Holland) for 30 min at 4°C. The resin was then washed four times with 20 ml wash buffer (50 mM Tris-Cl [pH 9.0], 400 mM KCl, 0.05% β-mercaptoethanol; for $ParR_{pCP301}$, pH 9.0; for $ParR_{pB171}$, pH 8.0) containing increasing concentrations (10 mM, 25 mM, 50 mM, and 100 mM) of imidazole. His-tagged ParR proteins were eluted in 5 ml of wash buffer containing 300 mM imidazole. Subsequently, the ParR-purified proteins were desalted using Econo-Pac 10DG columns (Bio-Rad) and eluted in 1 ml buffer S (50 mM Tris-Cl [pH 7.5], 250 mM NaCl, 1 mM EDTA, 1 mM DTT, 10% glycerol). For both ParR proteins, the approximate yield was 1 mg. $ParR_{pCP301}$ was determined to be >90% pure by SDS-PAGE, whereas $ParR_{pB171}$ was less pure due to the presence of a lower-molecular-weight contaminating band at approximately 30% of the intensity of $ParR_{pB171}$.

RESULTS

Plasmid partition incompatibility as a model system. We began by creating a system that would allow us to look for segregation-based plasmid incompatibility. Figure 1A depicts the R1 segregation system. ParM filaments are stabilized when each end interacts with one copy of the complex formed by the binding of multiple ParR dimers to *parC* DNA. To quantify the effect of Par operons on plasmid segregation, we engineered a plasmid (pEMH606) that used the replication origin of plasmid F1, lacked its own partitioning system, and carried β-galactosidase (LacZ) and chloramphenicol (Cm) resistance genes, allowing us to monitor its segregation both qualitatively (on media containing X-Gal, a chromogenic LacZ substrate) and quantitatively (by following the appearance of chloramphenicol-sensitive cells) (Fig. 1B). Consistent with previous studies (3), an R1-partitioning (Par) operon stabilized pEMH606 approximately 10^3-fold (Fig. 1C).

To determine the influence of its biological environment on pEMH606 stability, we introduced a second plasmid into the same cell and examined its effect on the segregation of pEMH606. The additional plasmid uses a higher-copy-number replication origin (*ori*MB1 from pMB1), which is fully compatible with *ori*F1 and confers kanamycin resistance. We call this the challenge plasmid and the lower-copy-number plasmid, which confers chloram-

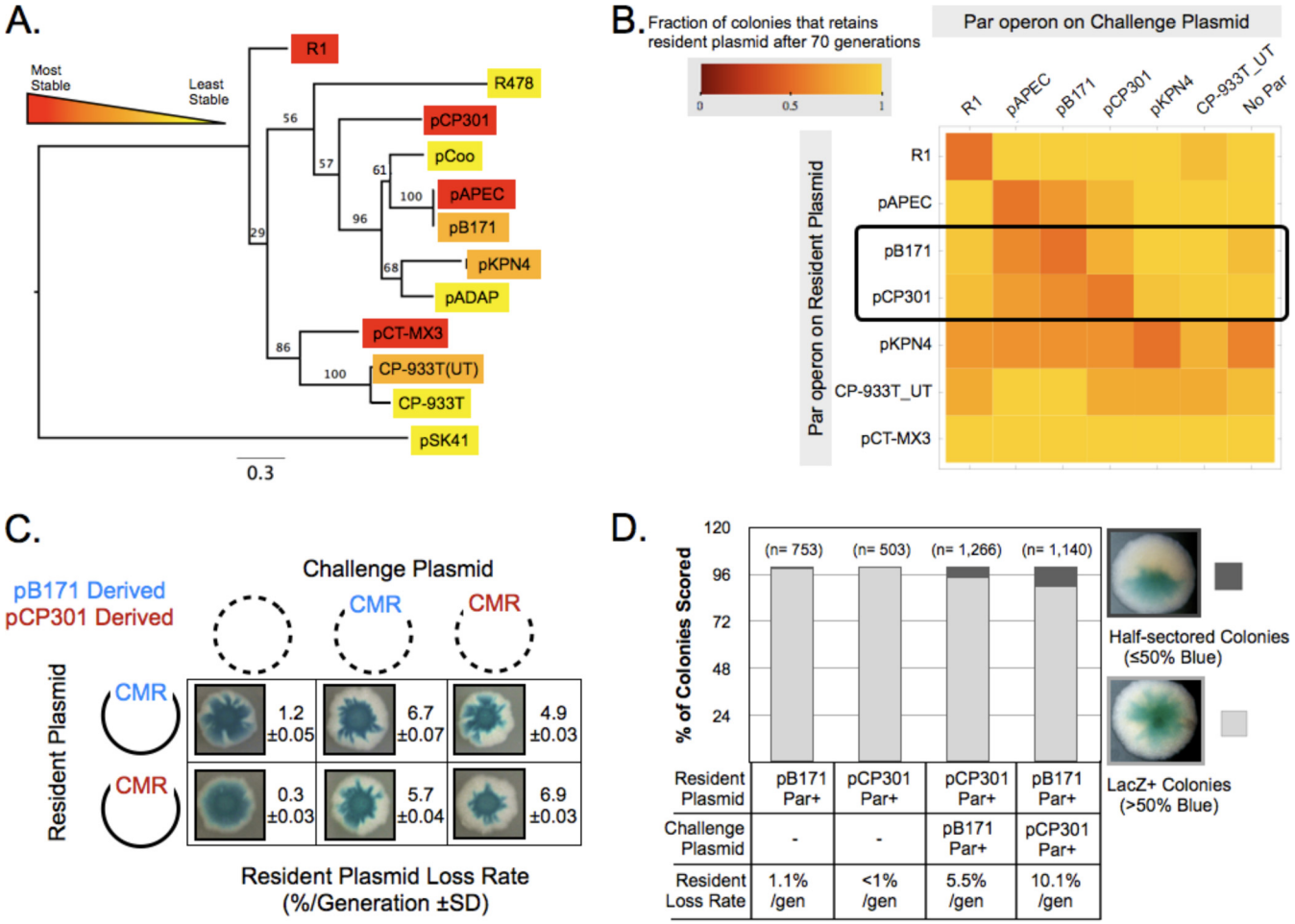

FIG 2 Limited plasmid partition incompatibility detected between type II partitioning homologs. (A) A maximum-likelihood-based phylogenetic tree of the ParM amino acid sequence of the type II partitioning operons utilized in this study, indicating the stability of resident plasmids containing them. Bootstrap values are shown. (B) A matrix displaying the results of quantitative compatibility assays for the indicated combinations of partitioning operons. Increasingly red squares indicate the levels of partition incompatibility observed. (C) Qualitative and quantitative incompatibility assay results showing the mutual incompatibility between Par_{pB171} and Par_{pCP301} plasmids. CMR, chloramphenicol resistance plasmid. (D) Direct detection of resident plasmid loss in the first cell division of a colony by the formation of half-sectored colonies for β-galactosidase expression. The plasmid pairs tested are indicated.

phenicol resistance and carries *ori*F1, the resident plasmid. Because the two replication origins are fully compatible, we can determine the effect of the challenge plasmid on the segregation of the resident plasmid by monitoring the loss rate of the resident plasmid in cells that are selected to maintain the challenge plasmid (see Fig. S1 in the supplemental material). Figure 1C shows both the qualitative and quantitative results of the incompatibility produced when both the resident plasmid and challenge plasmid carried the R1 Par operon: the challenge plasmid was destabilized at a level greater than 6-fold by the challenge plasmid carrying an intact segregation system but was unaffected when the challenge plasmid lacked a Par operon. This result demonstrates that we can measure the segregation incompatibility between plasmids and thus determine the relationship between genotype, phenotype, and fitness in a biologically and biochemically defined model system (Fig. 1D).

Plasmid partition incompatibility exists between two highly divergent partitioning operons. To investigate the linkage between genotype, phenotype, and fitness, we looked for cases of segregation incompatibility between homologous type II Par operons. Using the PFAM database entry for ParR (PF10784), we selected eleven "seed sequences," identified their associated ParM and *parC* sequences, and cloned the entire operon into the resident plasmid; for ParM, their amino acid identity with R1 ParM ranged from 21% (pSK41) to 47% (pCP-933T), and their pairwise identity with each other ranged from 17% to 99%. The host species for each of these plasmids, as well as that for the R1 plasmid, is listed in Table S1 in the supplemental material. Three operons (from plasmids pCP301, pAPEC, and pCT-MX3) behaved like R1 and conferred 10-fold stabilization. Three others (from pKPN4, pB171, and CP-933T_UT) stabilized the challenge plasmid to a lesser extent, and five (from pSK41, pADAP, pCoo, CP-933T, and R478) were nonfunctional (Fig. 2A). The phylogenetic relationship between the amino acid sequences of ParM, the most conserved component of these operons, is shown in Fig. 2A.

Next we sought to understand why particular heterologous Par operons failed to improve plasmid segregation or stabilized plasmids less well than the R1 *par* operon. We hypothesized that these defective Par operons (i) had acquired debilitating or loss-of-function mutations during the course of their evolution, (ii) re-

quire a host-specific factor(s) for partitioning function not found in *E. coli*, (iii) are inadequately expressed in *E. coli*, or (iv) have an indirect, unexpected effect on *oriF1* replication, thereby destabilizing the resident plasmid. Our data showed that the Par operons from pB171, pKPN4, pSK41, and pCoo did not negatively impact that stability of the mini-F1 plasmid lacking any partitioning operon, indicating that *ori*F1 replication was unaffected (not shown). We also found that expressing both ParR and ParM proteins at high levels from an additional plasmid did not assuage the impaired stabilization of pEMH606 by either pB171 or pKPN4 Par operons (not shown). This limited analysis might suggest that the suboptimal stabilization of pEMH606 by particular heterologous Par operons indicates that the products of these operons cannot function or be expressed in *E. coli* or, alternatively, that, in the absence of continued strong selection, they have accumulated mutations that reduce their ability to promote accurate partition. The observation that pB171 contains two partitioning operons is consistent with the second possibility (20).

We tested segregation compatibility by making resident and challenge plasmids with each of the seven functional operons, except pCT-MX3, which we were unable to clone into the high-copy-number plasmid. Every operon was strongly self-incompatible (Fig. 2B), but most pairs of operons were fully compatible (Fig. 2B). There were two types of exceptions. Resident plasmids carrying the pKPN4 or CP-933T_UT Par operons were destabilized by the majority of other Par operons. These plasmids were also destabilized by a challenge plasmid that lacks any partitioning sequence, so we conclude that their worse segregation was not due to interactions between the different Par operons. The molecular basis for this effect was not investigated further. The other interaction was specific incompatibility between the pCP301, pB171, and pAPEC Par operons. Because the Par operons of pAPEC and pB171 are almost identical and pB171 has been previously studied (20–22), we focused on the incompatibility between pCP301 and pB171 for the remainder of this study. The Par operons of pCP301 and pB171 mutually destabilize each other, raising the loss rate of the resident plasmid from ≤1% to about 5% (Fig. 2C).

We tested one potential caveat to our results, which depend on propagating a bacterial culture for 70 generations. If losing the resident plasmid allowed cells to divide faster, we would overestimate the rate of plasmid loss. To test this possibility, we used a method that directly detects the cell divisions in which plasmids were lost. When a colony arises from a single cell, a plasmid loss event at the first division produces a half-sectored colony: one half of the colony contains the plasmid, and one half does not. Because the resident plasmid carries the LacZ-encoding gene, the half of the colony that contains the plasmid would turn blue on X-Gal plates and the other half would remain white. Missegregation events that occur at a later division event produce colonies that are less than 50% white. With Par_{pB171} on the resident plasmid and Par_{pCP301} on the challenge plasmid, ~10% of the colonies were half-sectored, and the reciprocal experiment gave ~6% half-sectored colonies (Fig. 2D). These results show that the incompatibility between pB171 and pCP301 is not due to faster growth of cells that have lost plasmids and suggest that the serial transfer method slightly underestimates plasmid loss rates.

If plasmid incompatibility results from different plasmids being segregated from each other by the same ParM filaments, both plasmids from an incompatible pair must possess *parC*. To test this assertion, we made challenge plasmids that expressed ParR and ParM but lacked *parC*. These *parC*-less challenge plasmids did not destabilize Par_{pB171} or Par_{pCP301} resident plasmids (see Fig. S2 in the supplemental material), showing that incompatibility depends on the presence of *parC*, supporting the hypothesis that it arises through mixed pairing.

pB171 ParR protein binds productively to the pCP301 *parC* DNA sequence. To investigate the mechanism of partition incompatibility between Par_{pB171} and Par_{pCP301} plasmids, we engineered a series of six chimeric Par operons containing all combinations of ParM (pB171 gene identifier [ID] = 1238680, pCP301 = 1237997), ParR (gene ID pB171 = 1238681, pCP301 = 1237996) and *parC* from both plasmids (Fig. 3A). We reasoned that any chimera that stabilized a resident plasmid must have a functional *parC* and ParR interface and a functional ParR and ParM interface. Figure 3A shows that a chimera with ParR and ParM from pB171 and ParC from pCP301 ($M_{171}R_{171}C_{301}$) fully stabilized a resident plasmid. None of the other chimeras reduced the plasmid loss rate below 7%, and one, composed of pB171 ParR and *parC* and pCP301 ParM ($M_{301}R_{171}C_{171}$), made the resident plasmid segregate more poorly than it would have if all the plasmid molecules moved independently of each other (binomial partition).

The behavior of the $M_{171}R_{171}C_{301}$ chimera suggests that $ParR_{pB171}$ can bind to $parC_{pCP01}$, generating a protein and DNA complex that interacts with $ParM_{pB171}$ filaments to direct segregation. Therefore, we predicted that expressing only $ParR_{pB171}$ and $ParM_{pB171}$ from a second plasmid could stabilize a resident plasmid that carries only $parC_{pCP301}$. Figure 3B verifies this prediction, as the loss rate of the $parC_{pCP301}$ plasmid decreased from 7.4%/generation to 2.2%/generation when pB171 ParR and ParM proteins were coexpressed from a medium-strength promoter (P_{RNAI}) in the same cell.

To assess $ParR_{pB171}$ and $parC_{pCP01}$ binding *in vivo*, we exploited the findings that *parC* contains the Par promoter and that ParR binding to the *parC* represses transcription (23). We placed the gene for mKate (24), a monomeric RFP, downstream of *parC* and monitored mKate expression by fluorescence-activated cell sorting. In the absence of any ParR protein, $parC_{pCP301}$ drove strong mKate expression (Fig. 3C, upper panel), but cloning $ParR_{pCP301}$ or $ParR_{pB171}$ downstream of mKate reduced fluorescence 30- or 3-fold, respectively. A mutant of $ParR_{pB171}$ that eliminates DNA binding (*parR-K6E*) (22) alleviated repression (Fig. 3C, upper panel).

The interaction between heterologous ParR and *parC* is not reciprocal: the $M_{171}R_{171}C_{301}$ chimera fully stabilized the resident plasmid, whereas the $M_{301}R_{301}C_{171}$ chimera, carrying $parC_{pB171}$ DNA and encoding $ParR_{pCP301}$ and $ParM_{pCP301}$ proteins, did not. This result suggests that $ParR_{pCP301}$ cannot bind to $parC_{pB171}$ and support segregation. To probe this hypothesis, we designed similar mKate reporter constructs to probe transcriptional repression but instead drove expression from $parC_{pB171}$. Figure 3C (lower panel) shows that both $ParR_{pB171}$ and $ParR_{pCP301}$ produced roughly 2-fold repression of $parC_{pB171}$, suggesting that the requirements for transcriptional repression and plasmid segregation are not identical.

We next sought to verify the specificity of ParR and *parC* binding *in vitro* using a gel-shift assay. We purified His-tagged $ParR_{pB171}$ (NP_053129.1) and $ParR_{pCP301}$ (NP_858327.1) and monitored their ability to slow the electrophoretic gel mobility of *parC* DNA. Consistent with our analysis of transcriptional repression, both versions of ParR bound to both versions of *parC*. Nei-

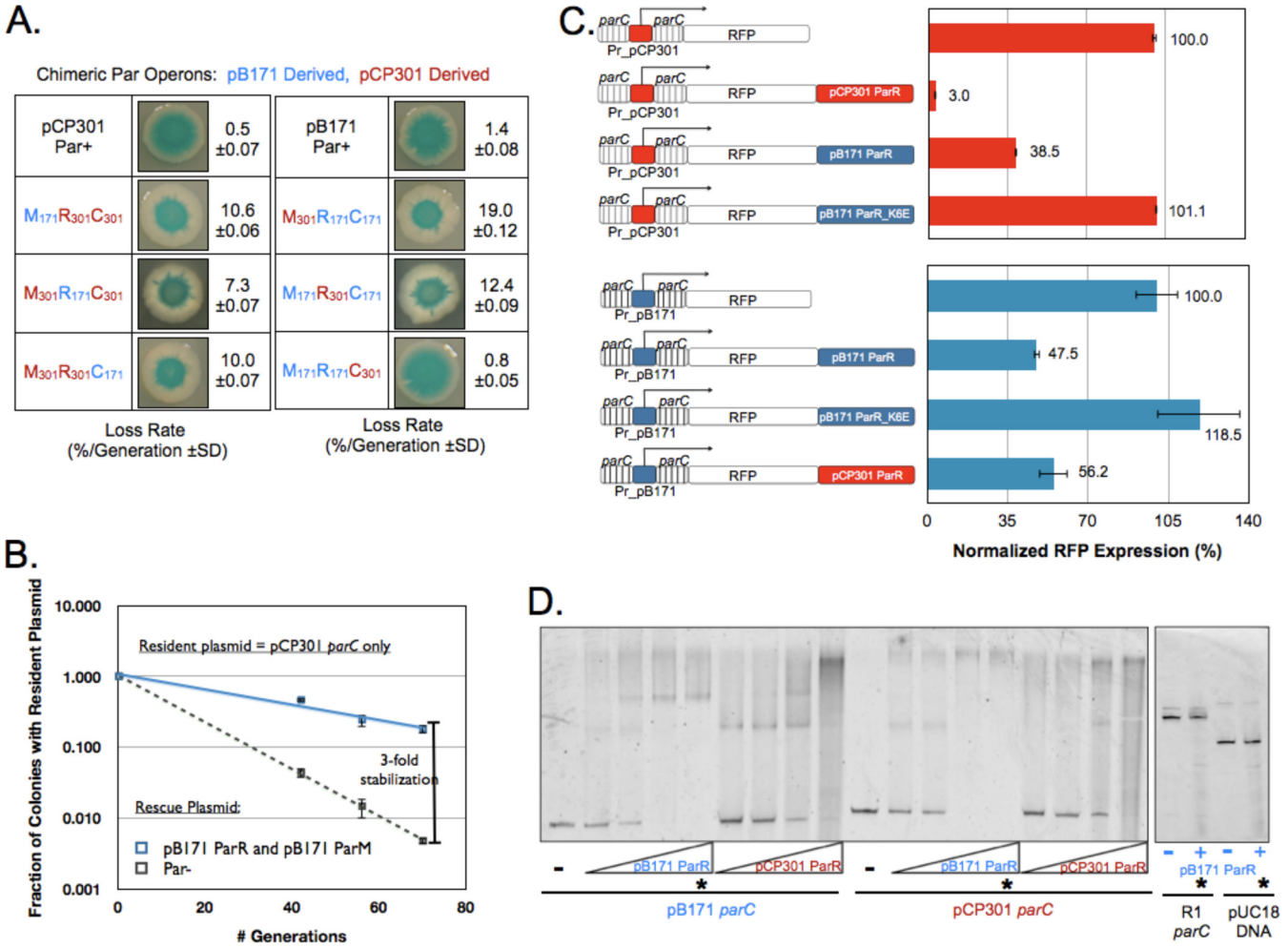

FIG 3 Cross talk between the pB171 and pCP301 Par operons occurs at the ParR and *parC* interface. (A) A chimera with $parC_{pCP301}$, $ParR_{pB171}$, and $ParM_{pB171}$ is stable. Data represent the results of qualitative and quantitative plasmid loss assays for resident plasmids carrying each of the 6 indicated chimeric operons as well as pB171 and pCP301 Par operons. (B) $ParR_{pB171}$ and $ParM_{pB171}$ stabilize resident plasmids containing only $parC_{pCP301}$. Data represent the results of quantitative plasmid loss assays for a resident plasmid carrying only $parC_{pCP301}$ in the presence of a rescue plasmid expressing either green fluorescent protein (GFP) (Par−) or $ParRM_{pB171}$ from a strong constitutive promoter. Error bars represent the 95% confidence intervals derived from two biological replicates, assayed in triplicate. (C) $ParR_{pB171}$ and $ParR_{pCP301}$ each cross repress the other's *parC*. Genetic structure of eight RFP reporters, with RFP expressed from either the pCP301 *parC* promoter (Pr_pCP301; red bars) or the pB171 *parC* promoter (Pr_pB171; blue bars). Data represent the mean fluorescence of each strain normalized to that of the strain containing the appropriate, nonrepressed RFP reporter. Error bars represent the 95% confidence intervals derived from six independent transformants of each reporter plasmid. (D) pCP301 and pB171 each bind the other's *parC in vitro*. Data represent the results of a gel shift assay to assess the ability of purified His-tagged $ParR_{pB171}$ and His-tagged $ParR_{pCP301}$ protein to bind to both $parC_{pB171}$ and $parC_{pCP301}$ DNA. Lanes marked with a star contain equal amounts of purified $ParR_{pB171}$ (8 μM) and a 2 nM concentration of the indicated DNA molecule. pUC18-derived DNA and $parC_{R1}$ act as nonspecific control DNA sequences.

ther $ParR_{pB171}$ nor $ParR_{pCP301}$ displayed detectable affinity for *parC* from a third plasmid (R1) or a control sequence derived from a standard cloning vector (pUC18) (Fig. 3D and data not shown).

A mixed-filament model can explain pCP301 and pB171 partition incompatibility. In the mixed-filament model of partitioning incompatibility, a plasmid with $parC_{pCP301}$ and a plasmid with $parC_{pB171}$, both bound by $ParR_{pB171}$, would be segregated from each other by a $ParM_{pB171}$ filament (Fig. 4A). The presence of multiple plasmids and multiple ParM filaments in small cells makes a rigorous test for these mixed filaments impossible. We therefore turned to simulation to ask whether formation of mixed filaments could explain our experimental data.

The model, shown in Fig. 4B, makes three key assumptions. The first is that preformed ParR complexes bind with first-order kinetics to *parC* and that the binding rate is the same for all possible interactions. As a result, the different affinities of ParR complexes for *parC* are determined only by differences in the off rate with which ParR dissociates from *parC*. The second is that ParM filaments can interact only with their cognate ParR complexes, and the third is that filament formation and extension along the long axis of the cell are instantaneous. Under these assumptions, the pattern of segregation is determined by which *parC*-containing plasmid molecules associate with a given ParR.

We used transcriptional repression to estimate the relative affinities of different forms of ParR for *parC*. Employing the reporter plasmid with RFP driven by *parC*, described earlier, we expressed $ParR_{pB171}$ or $ParR_{pCP301}$ constitutively from a second

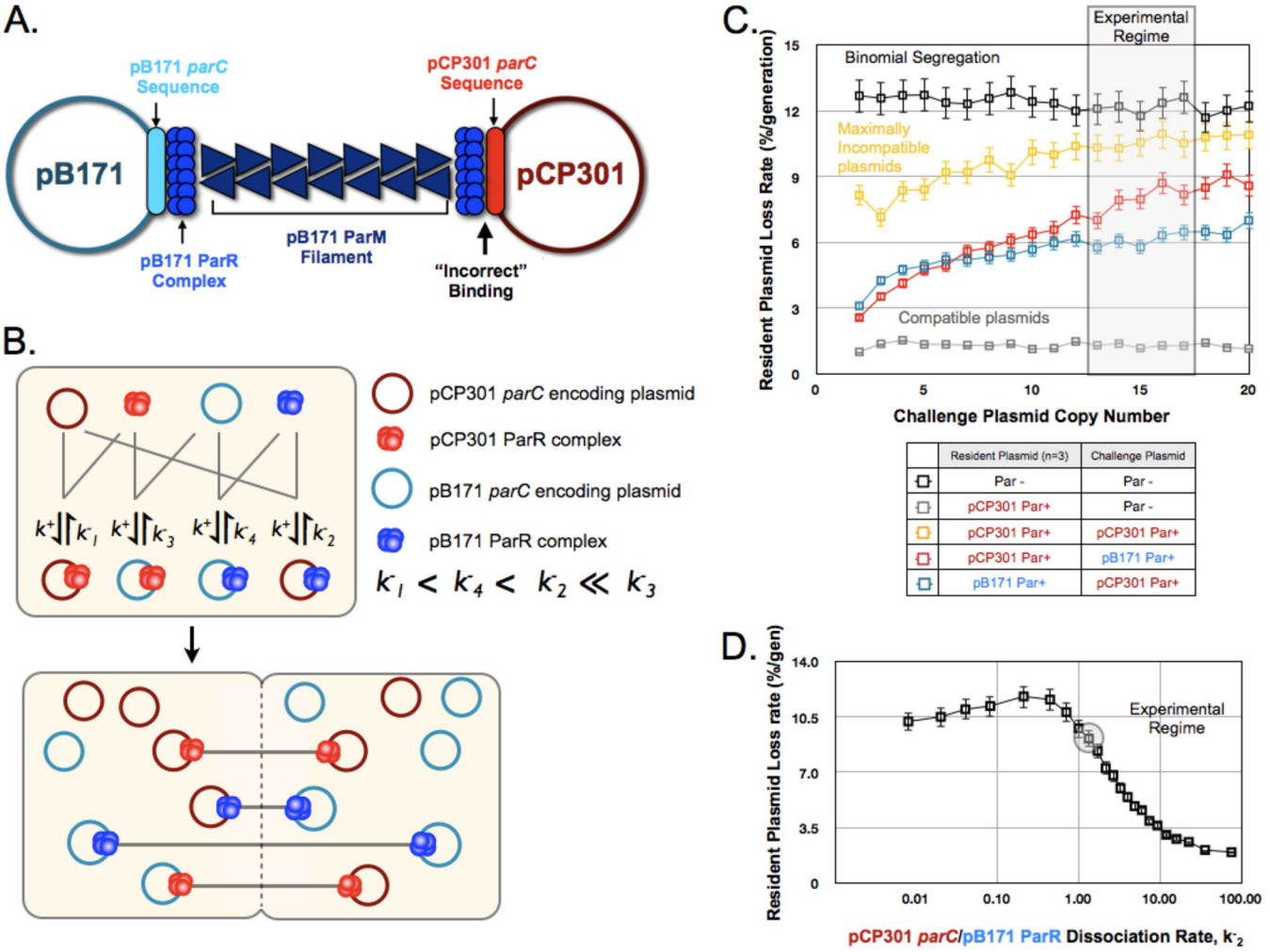

FIG 4 A mixed-filament model can explain plasmid partition incompatibility. (A) Schematic of the proposed mixed filaments formed in cells containing both Par_{pCP301} and Par_{pB171} plasmids, illustrating the "incorrect" binding of $ParR_{pB171}$ to $parC_{pCP301}$. (B) A two-step kinetic model for pB171 and pCP301 incompatibility based on the relative *in vivo* binding affinities of each ParR protein complex to both *parC* sequences. See the supplemental material for details. (C) Output from the simulations of plasmid partition incompatibility for the indicated combinations of plasmids, indicating the dependence of the resident plasmid (copy number = 3) loss rate on the copy number of the challenge plasmid. The region corresponding to the experimentally determined mean copy number of the *ori*MB1 challenge plasmid is shaded. Error bars represent 95% confidence intervals. (D) The dependence of the kinetic model for pCP301 and pB171 incompatibility on k^-_2, the dissociation rate of $ParR_{pB171}$ binding to $parC_{pCP301}$. The resident plasmid and challenge plasmid copy numbers were set at 3 and 15, respectively, and the experimentally approximated value for k^-_2 is highlighted. Error bars represent the 95% confidence interval.

plasmid and monitored fluorescence. Assuming that repression correlates with the level of ParR bound to *parC* and that ParR is not a limiting factor in the cell, these data yield the best approximation of the relative binding affinities for each pair of ParR and *parC* complexes (see Fig. S3 in the supplemental material), allowing us to assign relative off rates for the unbinding of different ParR proteins and *parC* sequences. Given these rates, we simulated partition incompatibility for 10,000 cells in parallel, using the Gillespie algorithm (25). At the end of the simulation, we paired plasmids bound by the same ParR protein and partitioned them to the two daughter cells, with each cell receiving one member of the pair. Unbound plasmids were assigned randomly to both cells with equal probabilities.

Figure 4C indicates the simulated loss rates for different combinations of resident and challenge plasmids. The resident plasmid was present at 3 copies per cell, and the copy numbers of the challenge plasmid differed. As the number of challenge plasmids increases, it gets harder for the resident plasmid to form an unmixed filament, and the loss rate of the resident plasmid rises. When two plasmids have the same Par operon (maximally incompatible), the resident plasmid's loss rate approaches the binomial loss rate at high copy numbers of the challenge plasmid.

We compared the simulation results to our experimental data. Quantitative PCR revealed that our resident plasmid was at about 3 copies/chromosome terminus (see Fig. S4 in the supplemental material), and the *ori*MB1 challenge plasmid is known to be maintained at ~15 copies/chromosome terminus (26). These values and our model predict a resident plasmid loss rate for Par_{pCP301} and Par_{pB171} plasmids of about 8%/generation, which is higher than the *in vivo* rate of about 5%/generation. This difference could reflect multiple factors, including greater discrimination in the formation of the complex that directs segregation, compared to

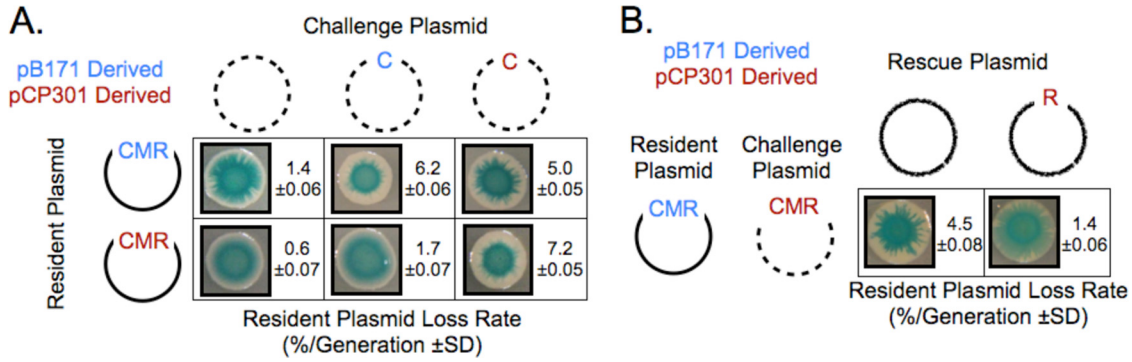

FIG 5 Partition incompatibility depends on competition between $ParR_{pB171}$ and $ParR_{pCP301}$ for binding to $parC_{pCP301}$. (A) Binding of $ParR_{pB171}$ to $parC_{pCP301}$ causes segregation incompatibility. Data represent the results of a quantitative and qualitative plasmid compatibility assay comparing a challenge plasmid carrying $parC_{pB171}$ to a challenge plasmid carrying $parC_{pCP301}$ with respect to the stability of Par_{pB171} or Par_{pCP301} resident plasmids. (B) Overexpression of $ParR_{pCP301}$ protects a Par_{pB171} resident plasmid from incompatibility. Data represent the results of quantitative and qualitative plasmid compatibility assays showing the incompatibility between a resident Par_{pB171} plasmid and a challenge Par_{pCP301} plasmid under conditions of constitutive expression of either GFP (Par^- plasmid) or $ParR_{pCP301}$ from a third plasmid.

our transcriptional repression measurements, and underestimation of the plasmid copy number.

Next, we investigated how robust the kinetic model was with respect to changes in the dissociation rate of the complex between $ParR_{pB171}$ and $parC_{pCP301}$ (k^-_2), the critical interaction that gives rise to our mixed filament. Over a 10-fold range, variation in k^-_2 switches the segregation of the resident plasmid from efficient ($k^-_2 = 10/s$) to barely better than binomial ($k^-_2 = 1/s$), indicating that this model of incompatibility is sensitive to k^-_2. Our estimate of k^-_2, 1.9/s, lies within this range. Furthermore, the modeled loss rate is insensitive to changes in the rate constant k^-_3, the dissociation constant of $ParR_{pCP301}$ and $parC_{pB171}$ complexes near these parameter values (see Fig. S5 in the supplemental material). This provides us with confidence that, similarly to the *in vivo* behavior, k^-_2 is the decisive parameter that governs incompatibility between Par_{pCP301} and Par_{pB171} plasmids.

Partition incompatibility reflects the interaction between pB171 ParR and pCP301 *parC*. The mixed-filament model for partition incompatibility makes testable predictions. The first is that a challenge plasmid that carries only *parC* can destabilize a resident plasmid with an intact Par operon, as was first shown for R1 (27). We predict that Par_{pB171} will be sensitive to a $parC_{pCP301}$ challenge plasmid, because $ParR_{pB171}$ can bind to $parC_{pCP301}$, producing mixed filaments linking resident and challenge plasmids. In contrast, Par_{pCP301} will be resistant to a $parC_{pB171}$ challenge plasmid because the binding of $ParR_{pCP301}$ to $parC_{pB171}$ is not productive for segregation. Figure 5A confirms these predictions: on its own, each Par_{pB171} plasmid and Par_{pCP301} plasmid is destabilized by its own *parC* on challenge plasmids, and Par_{pB171} is destabilized by a $parC_{pCP301}$ challenge plasmid, but Par_{pCP301} resists a $parC_{pB171}$ challenge plasmid.

The second prediction from our competition model is that incompatibility will be affected by changing the expression of the proteins involved in cross talk. In particular, we predict that increasing levels of $ParR_{pCP301}$ will help a resident plasmid with Par_{pCP301} resist a challenge from a Par_{pB171} plasmid: more $ParR_{pCP301}$ makes it harder for $ParR_{pB171}$ to bind $parC_{pCP301}$ and thus avoids the formation of mixed filaments. Figure 5C confirms the prediction: adding a third plasmid that expressed $ParR_{pCP301}$ stabilized the Par_{pCP301} resident plasmid 3-fold.

DISCUSSION

We used bacterial plasmid segregation to define the interactions between genotype, phenotype, and fitness. The partitioning machinery is simple, is entirely encoded by the plasmid, has minimal interactions with host proteins, and directly controls the propagation and thus the fitness of the plasmid. Related plasmids are analogous to related species and are from a common origin, with sequence similarities and differences in their segregation machinery affecting the degree of cross-reactivity. Compatible plasmids can coexist within a single cell and can be thought of as occupying different niches, whereas incompatible plasmids occupy the equivalent of overlapping niches and compete with each other. This competition means that the addition of an incompatible challenge plasmid alters the environment, phenotype, and fitness of a resident plasmid. Specifically, we uncovered the molecular basis of the mutual incompatibility between the Par operons derived from plasmids pB171 and CP301: the DNA-binding protein, $ParR_{pB171}$, can bind to the centromere-like *parC* of both plasmids, showing that accurate segregation in a cell with multiple plasmids depends on the specificity of the interaction between ParR and *parC*.

ParR plays two roles: it interacts with DNA to control the expression of the Par operon and forms a protein-DNA complex that binds to and modulates the dynamics of ParM filaments. *In vivo* analysis of transcriptional repression and *in vitro* analysis of DNA binding both show cross-reactivity between ParR and *parC* of the two plasmids. However, at the phenotypically critical level of plasmid segregation, the cross-reaction is unidirectional: binding of $ParR_{pB171}$ to $parC_{pCP301}$ can direct plasmid segregation, whereas the reciprocal reaction, the binding of $ParR_{pCP301}$ to $parC_{pB171}$, does not.

The molecular biology of ParR suggests reasons why cross-reactivity could be different for different aspects of plasmid behavior. Like $ParR_{R1}$, $ParR_{pB171}$ is a dimer in solution and binds cooperatively to its own *parC* DNA (20, 28). In both R1 and pB171, multiple ParR dimers bind to *parC*, making a ring-like protein-DNA complex (22, 29). In R1, this complex interacts with and stabilizes the ends of ParM filaments, and current models for filament elongation invoke multiple interactions between the ParM

filament and the ParR and ParC complex (9, 30). We speculate that the inability of the $parC_{pB171}$ and $ParR_{pCP301}$ complex to support partitioning is caused by too few $ParR_{CP301}$ dimers binding to $parC_{pB171}$.

Examining the sequence of *parC* does not offer an easy explanation for the ability of $ParR_{pB171}$ to direct the segregation of a plasmid bearing $parC_{pCP301}$. The sequence homology between pB171 and pCP301 *parC* is weak (see Fig. S6 in the supplemental material), and the consensus sequences that are believed to mediate the binding of $ParR_{pB171}$ to $parC_{pB171}$ are missing from $parC_{pCP301}$. Furthermore, the DNA-binding N-terminal regions of both $ParR_{pB171}$ and $ParR_{pCP301}$ show limited sequence identity (see Fig. S6) and are no more similar than the sequences of ParR proteins from compatible partitioning operons (22). Nevertheless, the ability of a mutation that prevents DNA binding to block the repressive activity of $ParR_{pB171}$ with respect to both $parC_{pB171}$ and $parC_{pCP301}$ demonstrates that DNA binding is required for the biological activity of ParR. Interestingly, the discriminator contacts that define the segregation specificity of plasmids encoding the type I Par operon, such as PI, have been mapped to an interaction between two hexameric sequences in the *parS* DNA and a 16-amino-acid stretch in the C terminus of the ParB protein (13, 14, 31–33). For the P1 plasmid, both these regions are dispensable for *parS* and ParB binding but are essential for mediating P1 segregation specificity (13). The limited sequence homology between *parC*/$ParR_{pB171}$ and *parC*/$ParR_{pCP301}$ (22) (see Fig. S6) suggests that the type II Par systems do not encode a similar discriminator that can distinguish different *parC* sequences, but further analyses would be required to rigorously test this possibility. Alternatively, other features of *parC* may be required to form the structure that directs plasmid segregation, such as the ability of *parC* DNA to easily bend into a ring-like *parC* and ParR complex or the spacing between the repetitive binding sites that might influence cooperativity between bound ParR dimers.

Our reductionist system succeeds in defining the basis for plasmid fitness in a given environment. The combination of simulation and genetic data show that cross talk at a single molecular interface, between ParR and *parC*, can cause inaccurate plasmid segregation. The binding of $ParR_{pB171}$ to $parC_{pCP301}$ is a failure to distinguish "self" from "nonself" on the part of both operons and means that both Par operons have reduced fitness when they end up in the same cell. If we think of incompatible plasmid pairs such as pB171 and pCP301 as belonging to the same group or "species" of plasmid, we can use the evolution of partition compatibility as a toy model for species determinations by identifying and characterizing mutations in the Par operon that make a pair of incompatible partitioning operons compatible, potentially by promoting specificity and self-recognition.

Is there selection for the evolution of plasmid compatibility? Our analysis focused on seven Par operons. Of these, three showed mutual incompatibility (with one pair very closely related in sequence), two showed Par-independent incompatibility, and the remaining two, R1 and pCT-MX3, were compatible with each other and with all the remaining operons. The sample was too small to permit general conclusions. Without better ecological knowledge on how often in nature plasmids encounter other plasmids within the same cell, we cannot tell where the truth lies between two extremes: whether plasmid compatibility results from selection for the divergence of replication and segregation machinery in plasmids that regularly cohabit and compete with each other or whether compatibility is the result of genetic drift in a simple molecular machine. The strong incompatibility, despite the high sequence divergence between the Par operons of pCP301 and pB171, argues for the latter possibility, but a combination of plasmid ecology and molecular dissection will be needed to produce a definitive answer. Nonetheless, we have established a model system that can be used to select for changes in molecular interfaces and to ask how these changes alter the fitness of genetic elements.

ACKNOWLEDGMENTS

We thank P. Malkus, J.-I. Bouet, N. Firth, K. Gerdes, D. Taylor, and G. Jagura-Burdzy for plasmids.

The simulations in this article were run on the Odyssey cluster supported by the FAS Science Division Research Computing Group at Harvard University.

This work was supported by a Charles A. King Trust postdoctoral fellowship (E.M.H.) and NIH grant RO1-GM43987 (A.W.M).

We thank M. Müller, R. Losick, and M. Laub for comments on the manuscript.

REFERENCES

1. **Watt WB.** 2013. Specific-gene studies of evolutionary mechanisms in an age of genome-wide surveying. Ann. N. Y. Acad. Sci. **1289:**1–17. http://dx.doi.org/10.1111/nyas.12139.
2. **Nordström K, Molin S, Aagaard-Hansen H.** 1980. Partitioning of plasmid R1 in Escherichia coli. I. Kinetics of loss of plasmid derivatives deleted of the par region. Plasmid **4:**215–227.
3. **Gerdes K, Molin S.** 1986. Partitioning of plasmid R1. Structural and functional analysis of the parA locus. J. Mol. Biol. **190:**269–279.
4. **Salje J, Gayathri P, Lowe J.** 2010. The ParMRC system: molecular mechanisms of plasmid segregation by actin-like filaments. Nat. Rev. Microbiol. **8:**683–692. http://dx.doi.org/10.1038/nrmicro2425.
5. **van den Ent F, Moller-Jensen J, Amos LA, Gerdes K, Lowe J.** 2002. F-actin-like filaments formed by plasmid segregation protein ParM. EMBO J. **21:**6935–6943. http://dx.doi.org/10.1093/emboj/cdf672.
6. **Choi CL, Claridge SA, Garner EC, Alivisatos AP, Mullins RD.** 2008. Protein-nanocrystal conjugates support a single filament polymerization model in R1 plasmid segregation. J. Biol. Chem. **283:**28081–28086. http://dx.doi.org/10.1074/jbc.M803833200.
7. **Salje J, Lowe J.** 2008. Bacterial actin: architecture of the ParMRC plasmid DNA partitioning complex. EMBO J. **27:**2230–2238. http://dx.doi.org/10.1038/emboj.2008.152.
8. **Garner EC, Campbell CS, Mullins RD.** 2004. Dynamic instability in a DNA-segregating prokaryotic actin homolog. Science **306:**1021–1025. http://dx.doi.org/10.1126/science.1101313.
9. **Gayathri P, Fujii T, Moller-Jensen J, van den Ent F, Namba K, Lowe J.** 2012. A bipolar spindle of antiparallel ParM filaments drives bacterial plasmid segregation. Science **338:**1334–1337. http://dx.doi.org/10.1126/science.1229091.
10. **Garner EC, Campbell CS, Weibel DB, Mullins RD.** 2007. Reconstitution of DNA segregation driven by assembly of a prokaryotic actin homolog. Science **315:**1270–1274. http://dx.doi.org/10.1126/science.1138527.
11. **Gerdes K, Moller-Jensen J, Bugge Jensen R.** 2000. Plasmid and chromosome partitioning: surprises from phylogeny. Mol. Microbiol. **37:**455–466. http://dx.doi.org/10.1046/j.1365-2958.2000.01975.x.
12. **Bouet JY, Nordstrom K, Lane D.** 2007. Plasmid partition and incompatibility–the focus shifts. Mol. Microbiol. **65:**1405–1414. http://dx.doi.org/10.1111/j.1365-2958.2007.05882.x.
13. **Radnedge L, Davis MA, Austin SJ.** 1996. P1 and P7 plasmid partition: ParB protein bound to its partition site makes a separate discriminator contact with the DNA that determines species specificity. EMBO J. **15:**1155–1162.
14. **Sergueev K, Dabrazhynetskaya A, Austin S.** 2005. Plasmid partition system of the P1par family from the pWR100 virulence plasmid of Shigella flexneri. J. Bacteriol. **187:**3369–3373. http://dx.doi.org/10.1128/JB.187.10.3369-3373.2005.
15. **Tobe T, Hayashi T, Han CG, Schoolnik GK, Ohtsubo E, Sasakawa C.** 1999. Complete DNA sequence and structural analysis of the enteropatho-

genic Escherichia coli adherence factor plasmid. Infect. Immun. **67:**5455–5462.
16. **Zhang J, Liu H, Zhang X, Yang J, Yang F, Yang G, Shen Y, Hou Y, Jin Q.** 2003. Complete DNA sequence and gene analysis of the virulence plasmid pCP301 of Shigella flexneri 2a. Sci. China C. Life. Sci. **46:**513–521. http://dx.doi.org/10.1360/02yc0060.
17. **Development Core Team R.** 2013. R: a language and environment for statistical computing. R Foundation for Statistical Computing, Vienna, Austria.
18. **Carapuça E, Azzoni AR, Prazeres DM, Monteiro GA, Mergulhão FJ.** 2007. Time-course determination of plasmid content in eukaryotic and prokaryotic cells using real-time PCR. Mol. Biotechnol. **37:**120–126. http://dx.doi.org/10.1007/s12033-007-0007-3.
19. **Skulj M, Okrslar V, Jalen S, Jevsevar S, Slanc P, Strukelj B, Menart V.** 2008. Improved determination of plasmid copy number using quantitative real-time PCR for monitoring fermentation processes. Microb. Cell Fact. **7:**6. http://dx.doi.org/10.1186/1475-2859-7-6.
20. **Ringgaard S, Ebersbach G, Borch J, Gerdes K.** 2007. Regulatory cross-talk in the double par locus of plasmid pB171. J. Biol. Chem. **282:**3134–3145. http://dx.doi.org/10.1074/jbc.M609092200.
21. **Ebersbach G, Gerdes K.** 2001. The double par locus of virulence factor pB171: DNA segregation is correlated with oscillation of ParA. Proc. Natl. Acad. Sci. U. S. A. **98:**15078–15083. http://dx.doi.org/10.1073/pnas.261569598.
22. **Møller-Jensen J, Ringgaard S, Mercogliano CP, Gerdes K, Löwe J.** 2007. Structural analysis of the ParR/parC plasmid partition complex. EMBO J. **26:**4413–4422. http://dx.doi.org/10.1038/sj.emboj.7601864.
23. **Jensen RB, Dam M, Gerdes K.** 1994. Partitioning of plasmid R1. The parA operon is autoregulated by ParR and its transcription is highly stimulated by a downstream activating element. J. Mol. Biol. **236:**1299–1309.
24. **Shcherbo D, Merzlyak EM, Chepurnykh TV, Fradkov AF, Ermakova GV, Solovieva EA, Lukyanov KA, Bogdanova EA, Zaraisky AG, Lukyanov S, Chudakov DM.** 2007. Bright far-red fluorescent protein for whole-body imaging. Nat. Methods **4:**741–746. http://dx.doi.org/10.1038/nmeth1083.
25. **Gillespie DT.** 2007. Stochastic simulation of chemical kinetics. Annu. Rev. Phys. Chem. **58:**35–55. http://dx.doi.org/10.1146/annurev.physchem.58.032806.104637.
26. **Covarrubias L, Cervantes L, Covarrubias A, Soberon X, Vichido I, Blanco A, Kupersztoch-Portnoy YM, Bolivar F.** 1981. Construction and characterization of new cloning vehicles. V. Mobilization and coding properties of pBR322 and several deletion derivatives including pBR327 and pBR328. Gene **13:**25–35.
27. **Dam M, Gerdes K.** 1994. Partitioning of plasmid R1. Ten direct repeats flanking the parA promoter constitute a centromere-like partition site parC, that expresses incompatibility. J. Mol. Biol. **236:**1289–1298.
28. **Møller-Jensen J, Borch J, Dam M, Jensen RB, Roepstorff P, Gerdes K.** 2003. Bacterial mitosis: ParM of plasmid R1 moves plasmid DNA by an actin-like insertional polymerization mechanism. Mol. Cell **12:**1477–1487. http://dx.doi.org/10.1016/S1097-2765(03)00451-9.
29. **Hoischen C, Bussiek M, Langowski J, Diekmann S.** 2008. Escherichia coli low-copy-number plasmid R1 centromere parC forms a U-shaped complex with its binding protein ParR. Nucleic Acids Res. **36:**607–615. http://dx.doi.org/10.1093/nar/gkm672.
30. **Schumacher MA, Glover TC, Brzoska AJ, Jensen SO, Dunham TD, Skurray RA, Firth N.** 2007. Segrosome structure revealed by a complex of ParR with centromere DNA. Nature **450:**1268–1271. http://dx.doi.org/10.1038/nature06392.
31. **Youngren B, Radnedge L, Hu P, Garcia E, Austin S.** 2000. A plasmid partition system of the P1-P7par family from the pMT1 virulence plasmid of Yersinia pestis. J. Bacteriol. **182:**3924–3928. http://dx.doi.org/10.1128/JB.182.14.3924-3928.2000.
32. **Dabrazhynetskaya A, Brendler T, Ji X, Austin S.** 2009. Switching protein-DNA recognition specificity by single-amino-acid substitutions in the P1 par family of plasmid partition elements. J. Bacteriol. **191:**1126–1131. http://dx.doi.org/10.1128/JB.01358-08.
33. **Dabrazhynetskaya A, Sergueev K, Austin S.** 2005. Species and incompatibility determination within the P1par family of plasmid partition elements. J. Bacteriol. **187:**5977–5983. http://dx.doi.org/10.1128/JB.187.17.5977-5983.2005.